Earthline Journal of Chemical Sciences
E-ISSN: 2581-9003; CODEN: EJCSB4
Volume 13, Number 4, November 2026, Pages 357-375
https://doi.org/10.34198/ejcs.13426.25.357375

Interaction of nitronium ion with BN-bond embedded phenanthrenes – A DFT treatment

Lemi Türker

Department of Chemistry, Middle East Technical University, Üniversiteler, Eskişehir Yolu No: 1, 06800 Çankaya/Ankara, Turkey
e-mail: lturker@gmail.com; lturker@metu.edu.tr

Abstract

In recent years, boron–nitrogen heteroarenes possess great promise for practical application in many areas of chemistry, biochemistry and pharmacology, beside materials science, and transition-metal-based catalysis. Presently, interaction of B-N bond embedded phenanthrene isomers with the nitronium ion are investigated within the constraints of density functional theory (DFT) at the level of B3LYP/6-31++G(d,p). The collected data have revealed that the optimized structures of them have exothermic heats of formation and favorable Gibbs free energy of formation values. They are thermally favored and electronically stable at the standard states. Various structural and quantum chemical data have been collected and discussed, including bond densities and time dependent density functional UV-VIS spectra.

1. Introduction

The replacement of two carbon atoms in a benzene ring with one boron and one nitrogen atom can proceed according to three permutations to produce 1,2-dihydro-1,2-azaborine, 1,3-dihydro-1,3-azaborine, or 1,4-dihydro-1,4-azaborine.

The total electronic number of two carbons (12e) is equal to the electronic sum of one boron (5e) and one nitrogen (7e). Accordingly, replacing two carbons with one boron and one nitrogen in a π-conjugated structure gives an isoelectronic system, i.e., the BN perturbed π-conjugated system, comparing to their all-carbon analogs. The electronic configuration of boron is $1s^2\ 2s^2\ 2p^1$. Its trivalency is explained by promoting the electrons from 2s to 2p orbitals, so that the number of unpaired electrons becomes three. Then, one 2s and two 2p orbitals are hybridized to form a set of three equivalent sp^2 hybrid orbitals which are triangular planar, with a bond angle of 120°.

For B-N covalent bond embedded π-conjugated units, they are suitable to act as electron-rich units to construct electron-donor materials owing to their high-lying energy levels, good backbone co-planarity, and high hole mobility. However, their absorption bands should be further broadened to lower energy (600–800 nm) to enhance the light harvesting ability [1].

Most trivalent boron reagents are eletrophiles owing to the vacancy for two electrons to fill the outer orbital of boron; however, interestingly, trivalent boron compounds can change their electrophilic character to a nucleophilic character by only changing the nature of the substituents on the boron atoms. With the help of computational tools, researchers have analyzed the structural- and electronic properties of boryl fragments that were either bonded to main-group metals or coordinated to transition-metals/rare-earth-metals and the same researchers have designed a map that might help to identify certain trends. This trend map will be useful for selecting an appropriate trivalent boron compound, depending on the sought reactivity [2,3].

Received: August 9, 2026; Accepted: September 7, 2026; Published online: September 14, 2026

Keywords and phrases: BN-bond embedded phenanthrenes, nitronium ion, isoelectronic structure, UV-VIS spectra, DFT calculations.

Among aromatic compounds, borazaenes represent a significant class of isosteres in which carbon-carbon bonds have been replaced by B−N bonds. Boron–nitrogen heteroarenes hold great promise for practical application in many areas of chemistry, such as BN-heterocycles in biochemistry and pharmacology, materials science, and transition-metal-based catalysis, etc. [4].

Boron-containing compounds have a wide range of structures and rich and multifaceted reactivity patterns. As a result, these compounds are being increasingly used in organometallic, supramolecular, organic and inorganic chemistry, as well as in catalysis and materials science. This perspective describes recent ground-breaking studies and their implications for the future development of new catalysts and materials containing one or several trivalent boron atoms [5].

For B-N covalent bond embedded π-conjugated units, they are suitable to act as electron-rich units to construct electron-donor materials owing to their high-lying energy levels, good backbone co-planarity, and high hole mobility. However, their absorption bands should be further broadened to lower energy (600–800 nm) to enhance the light harvesting ability [1]. Various theoretical and experimental studies are present in the literature involving B-N bond containing systems [5-10].

In the present study, interaction of B-N bond embedded phenethrene isomers with the nitronium ion are investigated within the constraints of density functional theory (DFT).

2. Method of Calculations

In the present study, all the initial optimizations of the structures leading to energy minima have been achieved first by using MM2 method which is then followed by semi empirical PM3 self consistent fields molecular orbital method [11-13]. Afterwards, the structure optimizations have been achieved within the framework of Hartree-Fock and finally by using density functional theory (DFT) at the level of B3LYP/6-31++G(d,p) [14,15]. Note that the exchange term of B3LYP consists of hybrid Hartree-Fock and local spin density (LSD) exchange functions with Becke's gradient correlation to LSD exchange [16]. The correlation term of B3LYP consists of the Vosko, Wilk, Nusair (VWN3) local correlation functional [17] and Lee, Yang, Parr (LYP) correlation correction functional [18]. In the present study, the normal mode analysis for each structure yielded no imaginary frequencies for the $3N–6$ vibrational degrees of freedom, where N is the number of atoms in the system. This search has indicated that the structure of each molecule considered corresponds to at least a local minimum on the potential energy surface. Furthermore, all the bond lengths have been thoroughly searched in order to find out whether any bond cleavages occurred or not during the geometry optimization process. All these computations were performed by using SPARTAN 06 program [19].

3. Results and Discussion

Phenanthrene is an even alternant hydrocarbon having equal numbers of starred and unstarred positions (topologically) and symmetrical molecular orbital energy spectrum about the zero energy level [20,21]. When centric perturbations occur to replace the skeletal carbons with some heteroatoms, molecular orbital energies (occupied and unoccupied) change. Generally, electron attracting atoms lower and electron donors raise the molecular orbital energy levels [20,21]. In the case of B-N bond insertion, boron and nitrogen have opposite effects on the molecular orbital energy levels [21]. The effect of a B-N bond in a conjugated system, like phenanthrene, is also affected by the position of its insertion [22].

Figure 1 shows the optimized structures of the systems of consideration. The arrows stand for the direction

of calculated dipole moment vectors. Note that a resultant dipole moment vector of a molecule is the vectorial sum of the individual bond dipoles, thus location of the heteroatoms greatly affects both the magnitudes and the directions. Initial structure of G resisted to optimization. So, the structure in Figure 1 for it just gives an idea about the connectivity of the atoms. As seen in the figure, the site of attack/conformation of the nitronium ion is determined by the nucleophilic position of the phenanthrene molecule which has been the electron distribution caused by the perturbation by BN bond. The other interactions such as charge-charge, dipole-dipole, and charge-dipole even possible secondary orbital interactions may have some contributions.

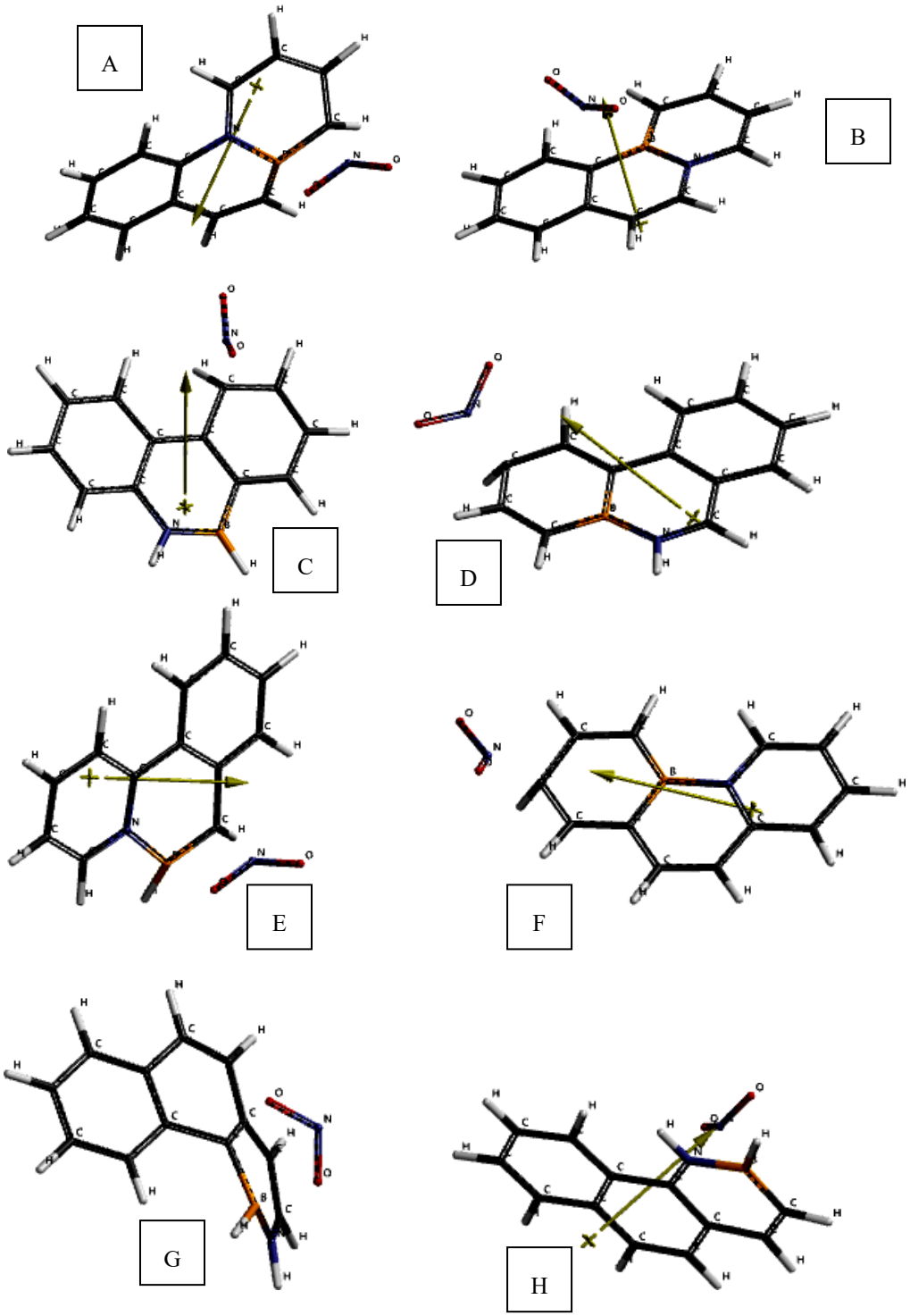

Figure 1. Optimized structures of the species considered (except G).

Some thermo chemical properties of the structures considered are listed in Table 1. The data presented in the table reveal that the standard thermo chemical formation data of all the species considered are exothermic (H^o values) and they are favored according to their G^o (Gibbs free energy of formation) values. The algebraic orders of H^o and G^o values are E<D<F=H<C<B<A and E<D<F=H<C<A<B, respectively. Note that they are all isomeric structures thus the scatter observed should be due to overall topological factors (gross and fine) operating on the systems of consideration.

Table 1. Some thermo chemical properties of the structures considered.

Species	H^o	S^o (J/mol^o)	G^o
A	-1962837.604	432.34	-1962966.507
B	-1962787.761	446.35	-1962920.844
C	-1962872.028	434.17	-1963001.479
D	-1962906.469	436.06	-1963036.483
E	-1962951.962	424.95	-1963078.662
F	-1962876.691	435.62	-1963006.570
H	-1962876.691	435.62	-1963006.570

Energies in kJ/mol.

Some energies of the structures considered are included in Table 2, where E, ZPE and E_C stand for the total electronic energy, zero point vibrational energy and the corrected total electronic energy, respectively. According to the data, all the structures are electronically stable. The order the stabilities are E>D>F>C>H>A>B.

Table 2. Some energies of the structures considered.

Species	E	ZPE	E_C
A	-1963392.00	540.37	-1962851.63
B	-1963338.13	534.52	-1962803.61
C	-1963425.77	539.63	-1962886.14
D	-1963463.50	542.87	-1962920.63
E	-1963507.42	542.60	-1962964.82
F	-1963432.03	541.25	-1962890.78
H	-1963392.96	533.38	-1962859.58

Energies in kJ/mol.

Figure 2 shows the calculated bond lengths of the structures considered.

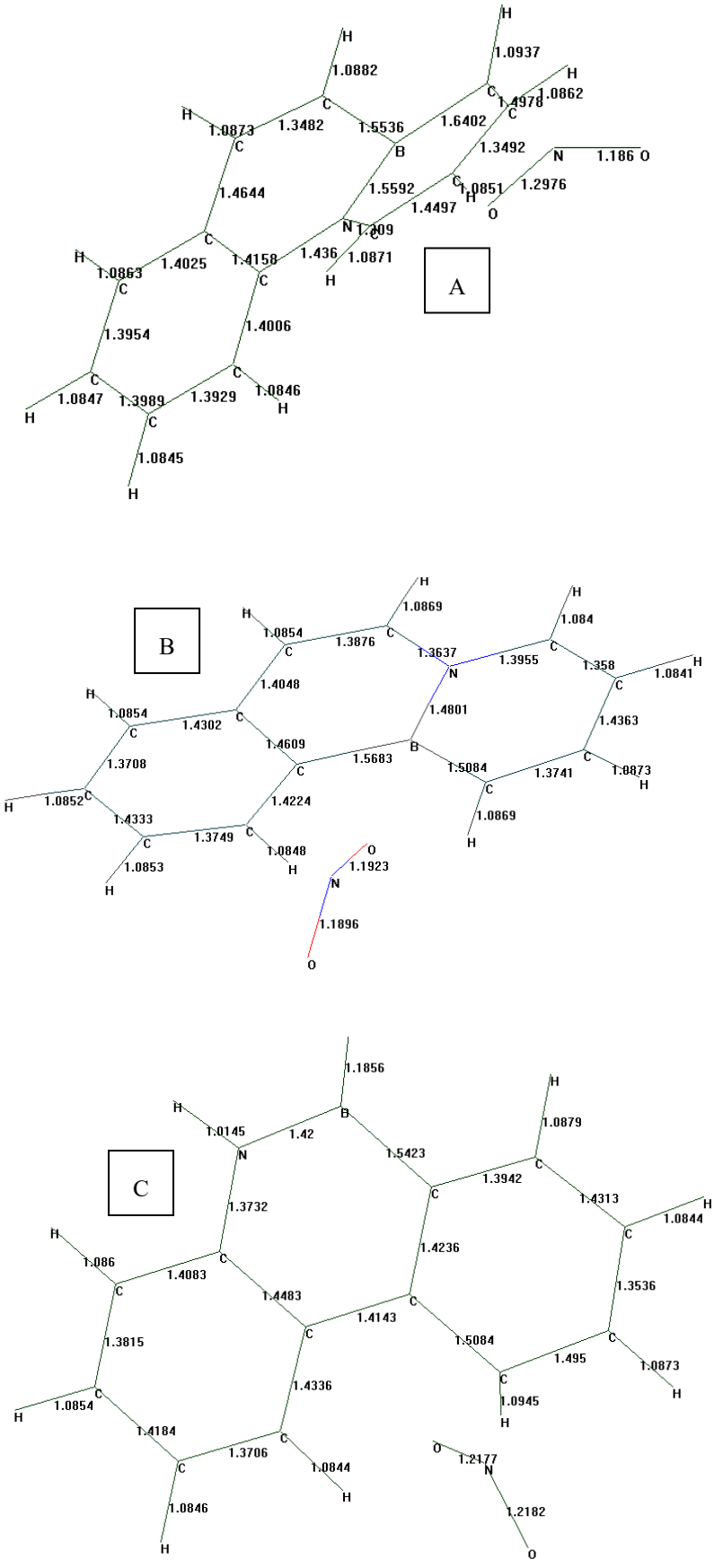

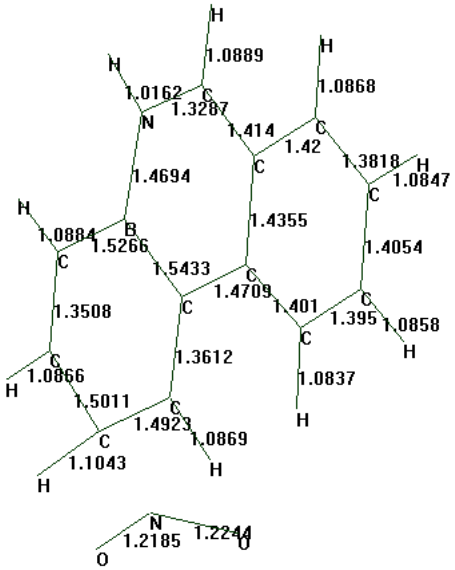
H
1.0889
H
1.0162
C
1.3287
N
1.414
H
1.0868
C
1.42
C
1.3818
H
1.0847
C
1.4694
H
1.0884
B
1.5266
C
1.4355
1.4054
1.5433
C
1.4709
1.401
C
1.395
1.0858
H
1.3508
C
1.3612
C
1.0866
H
1.0837
H
1.5011
C
1.4923
1.0869
C
1.1043
H
H
N
1.2185
1.2244
O
O

D

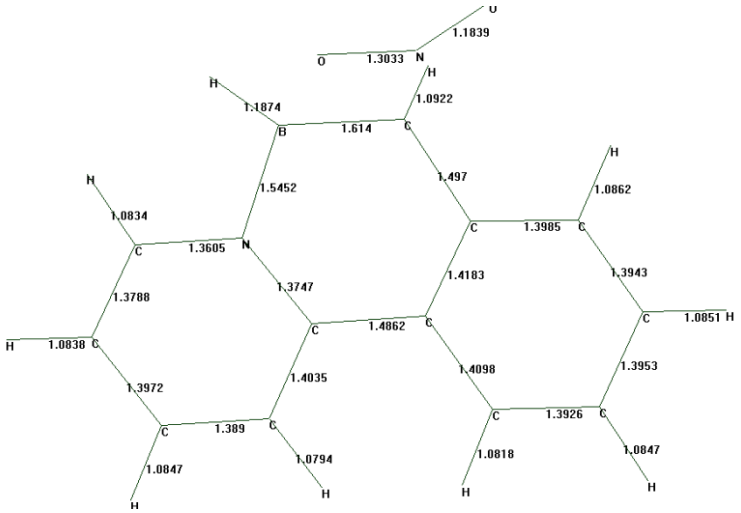
O
1.1839
O
1.3033
N
H
1.0922
H
1.1874
B
1.614
C
1.497
H
1.0862
H
1.0834
1.5452
C
1.3985
C
C
1.3605
N
1.3747
1.4183
1.3943
1.3788
C
1.4862
C
1.0851
H
H
1.0838
C
1.4098
1.3953
1.4035
1.3972
C
1.3926
C
C
1.389
C
1.0818
1.0847
1.0794
1.0847
H
H
H

E

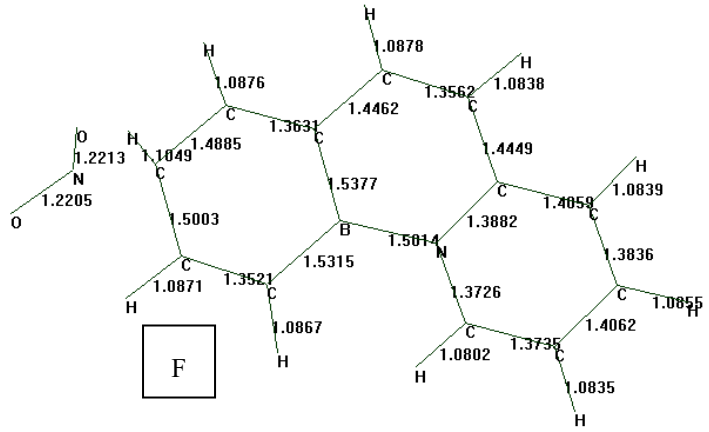
H
1.0878
H
1.0876
C
1.3562
H
1.0838
C
1.4462
C
1.3631
O
H
1.4885
1.4449
1.2213
1.1049
C
1.5377
H
1.0839
N
1.2205
C
1.4059
C
1.5003
1.3882
B
1.5014
N
1.3836
C
1.5315
1.0871
1.3521
C
1.3726
C
1.0855
H
H
1.0867
C
1.4062
1.0802
1.3735
C
H
1.0835
H

F

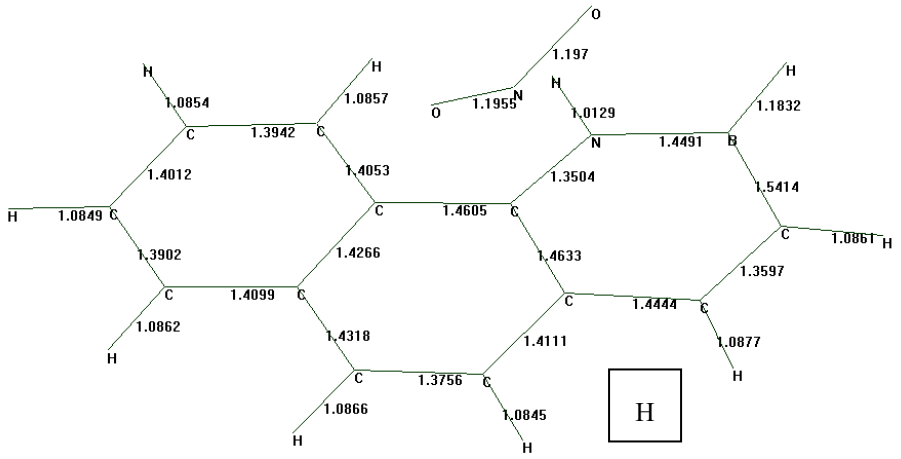

Figure 2. The calculated bond lengths of the structures considered.

The shortest B-N bond happens in structure-C (1.42 Å) whereas the longest in structure-A (1.55 Å).

Figure 3 displays the electrostatic potential maps of the species presently considered. Note that electro static potential is the energy of interaction of a positive charge with the nuclei and fixed electron distribution of a molecule [19]. In an electrostatic potential map negative potential regions reside on red/reddish and positive ones on blue/bluish parts of the maps. As seen in the figure, in each case the positive charge of the nitronium ion, affects the whole system, thus the local effects are veiled.

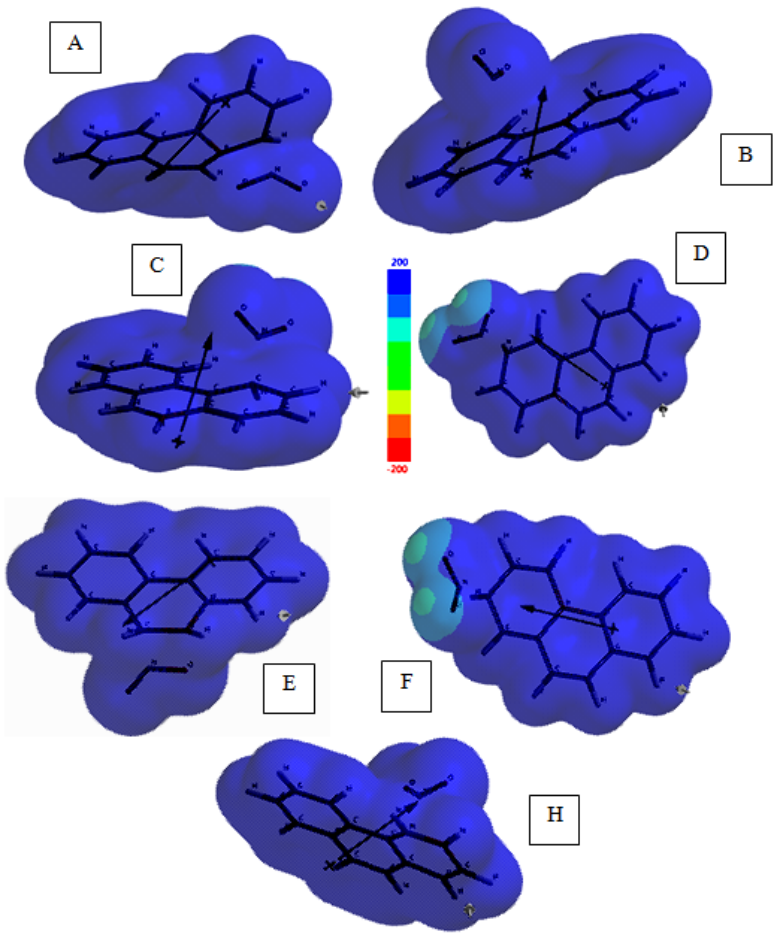

Figure 3. Electrostatic potential maps of the species presently considered.

Figure 4 displays the ESP charges on the atoms of the structures considered. The ESP charges are obtained by the program based on a numerical method that generates charges that reproduce the electrostatic potential field from the entire wavefunction [19]. Figure 4 reveals that ESP charge of the boron atom is always positive. Thus, the adjacent atoms (mainly carbons, nitrogen and in some cases also hydrogen) have negative partial charges.

The π-conjugation of parent phenanthrene skeleton is perturbed in various extents by the presence of heteroatoms depending on the location of the centric perturbations have occurred. Thus the charges and bond lengths in the structures are highly dependent on the fine topologies of the systems considered (see Figures 2 and 4).

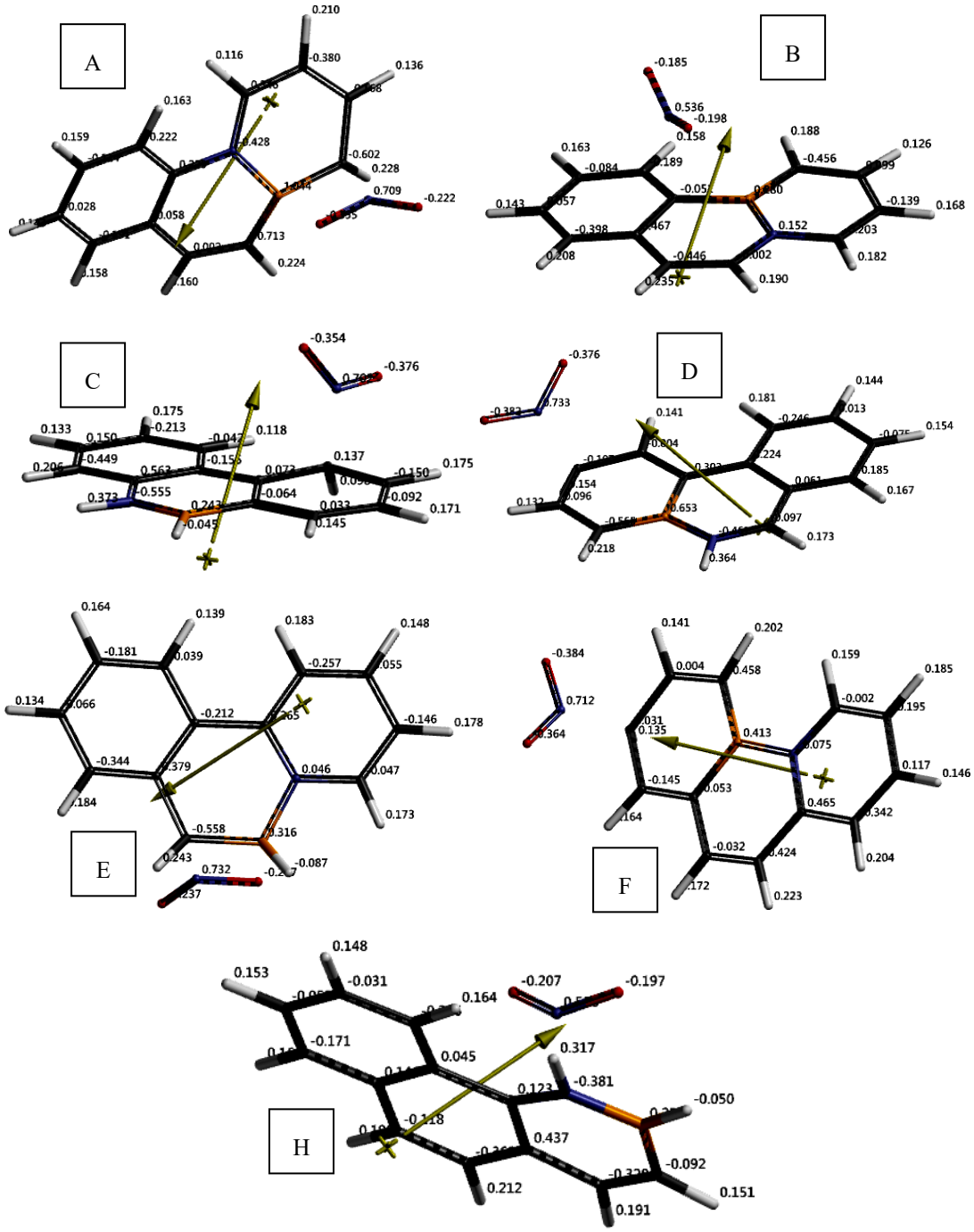

Figure 4. ESP charges on atoms of the species presently considered.

The local ionization potential maps of the species presently considered are shown in Figure 5. The presence of the nitronium ion deprives the organic part totally electron deficient. It is worth noting that local ionization potential is a measure of the relative ease of electron removal (ionization) as a function of localization [19,23]. Figure 5 shows the local ionization potential maps of the species where conventionally red/reddish regions (if any exists) on the density surface indicate areas from which electron removal is relatively easy, meaning that they are subject to electrophilic attack. Note that the local ionization potential map is a graph of the value of the local ionization potential on an isodensity surface corresponding to a van der Waals surface [19,23].

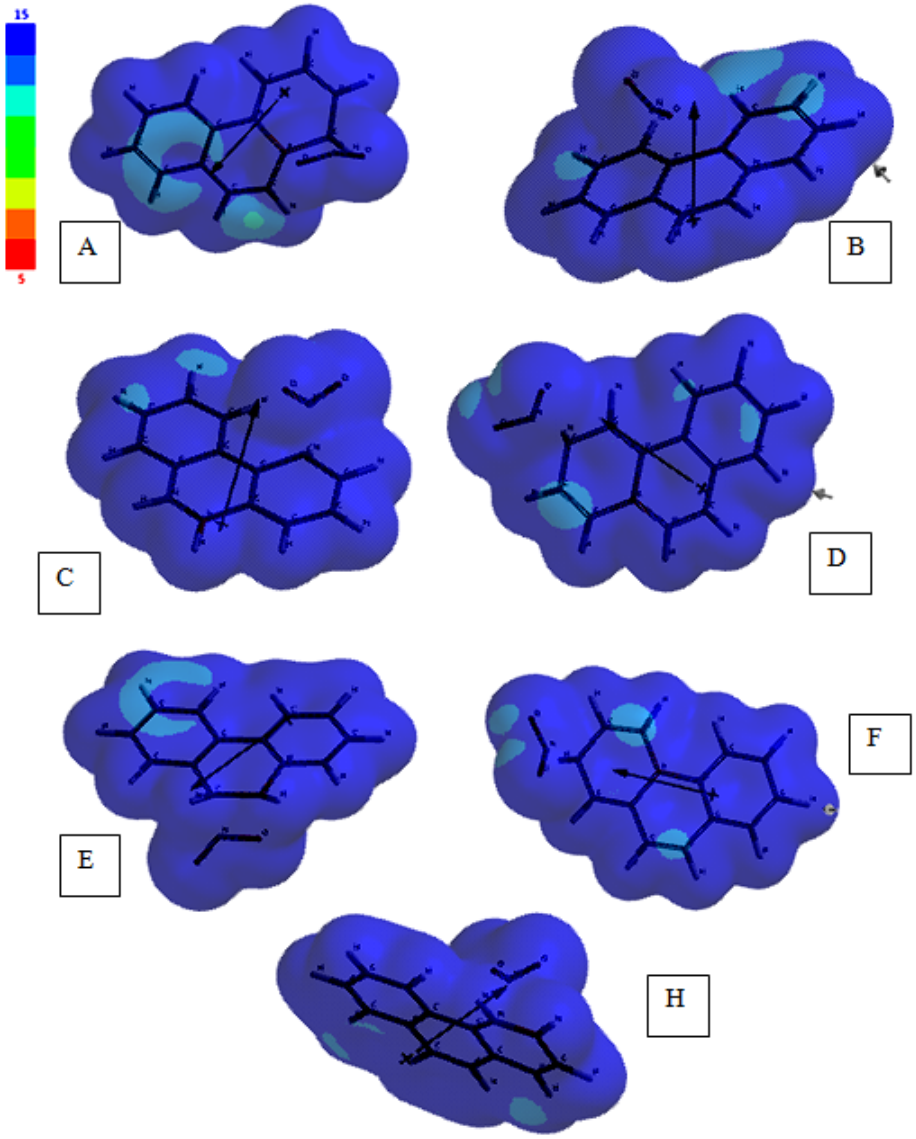

Figure 5. Local ionization potential maps of the species presently considered.

Figure 6 shows the LUMO maps of the species presently considered. A LUMO map displays the absolute value of the LUMO on the electron density surface. The blue color (if any exists) stands for the maximum value of the LUMO and the red colored region, associates with the minimum value. It is to be noted that the LUMO and NEXTLUMO (LUMO+1) are the major orbitals directing the molecule towards the attack of nucleophiles [19,23]. Positions where the greatest LUMO coefficient exists is the most vulnerable site in nucleophilic reactions.

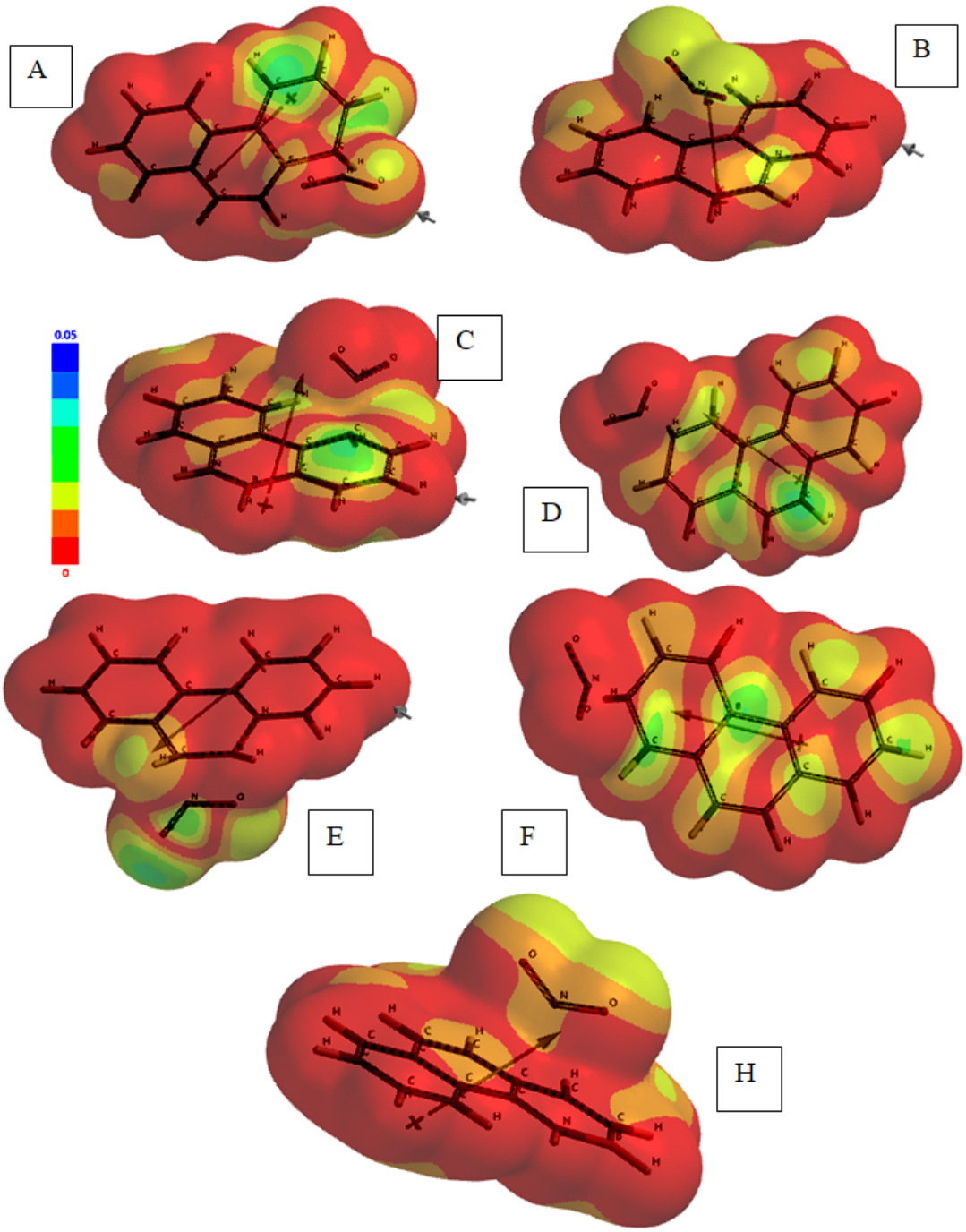

Figure 6. LUMO maps of the species presently considered.

Figure 7 stands for the bond density maps of the species considered. The bond density contains fewer electrons in total and demarks atomic connectivity. Figure clearly indicates that except the case of B and H, there exit some sorts of strong bonding interaction between the nitronium ion and the organic component. Although, in the cases of C, D and F it is mainly via the nitrogen atom of the nitronium ion and the boron atom does not participate at all, in A and E it does through a bicentric interaction with the organic moiety.

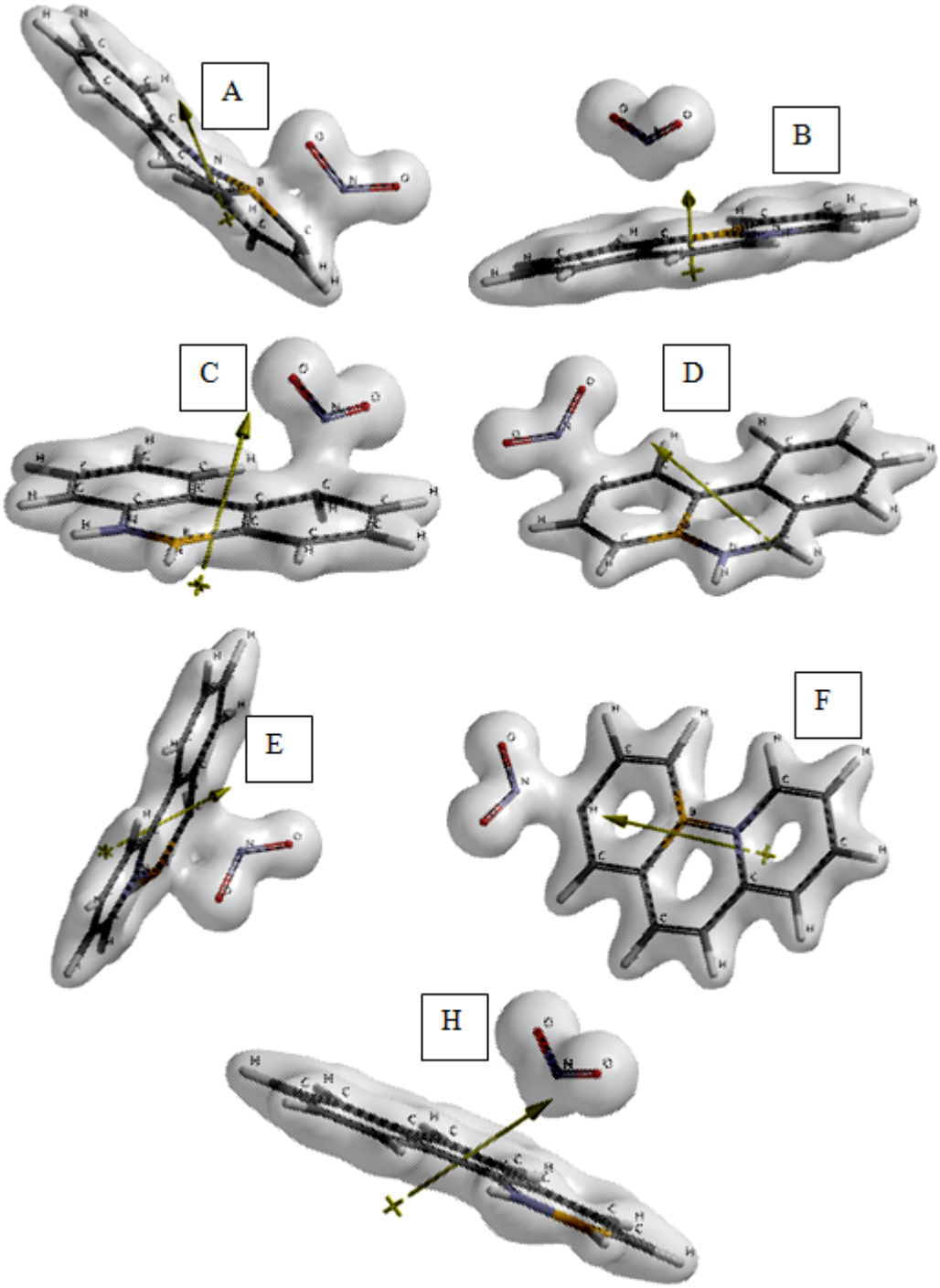

Figure 7. Bond density maps of the species considered.

Figure 8 displays some of the molecular orbital energy levels of the species, whereas Table 3 lists the HOMO, LUMO energies and Δε values (frontier molecular orbital energy gap, $\Delta\varepsilon = \varepsilon_{LUMO}-\varepsilon_{HOMO}$) values of the species considered.

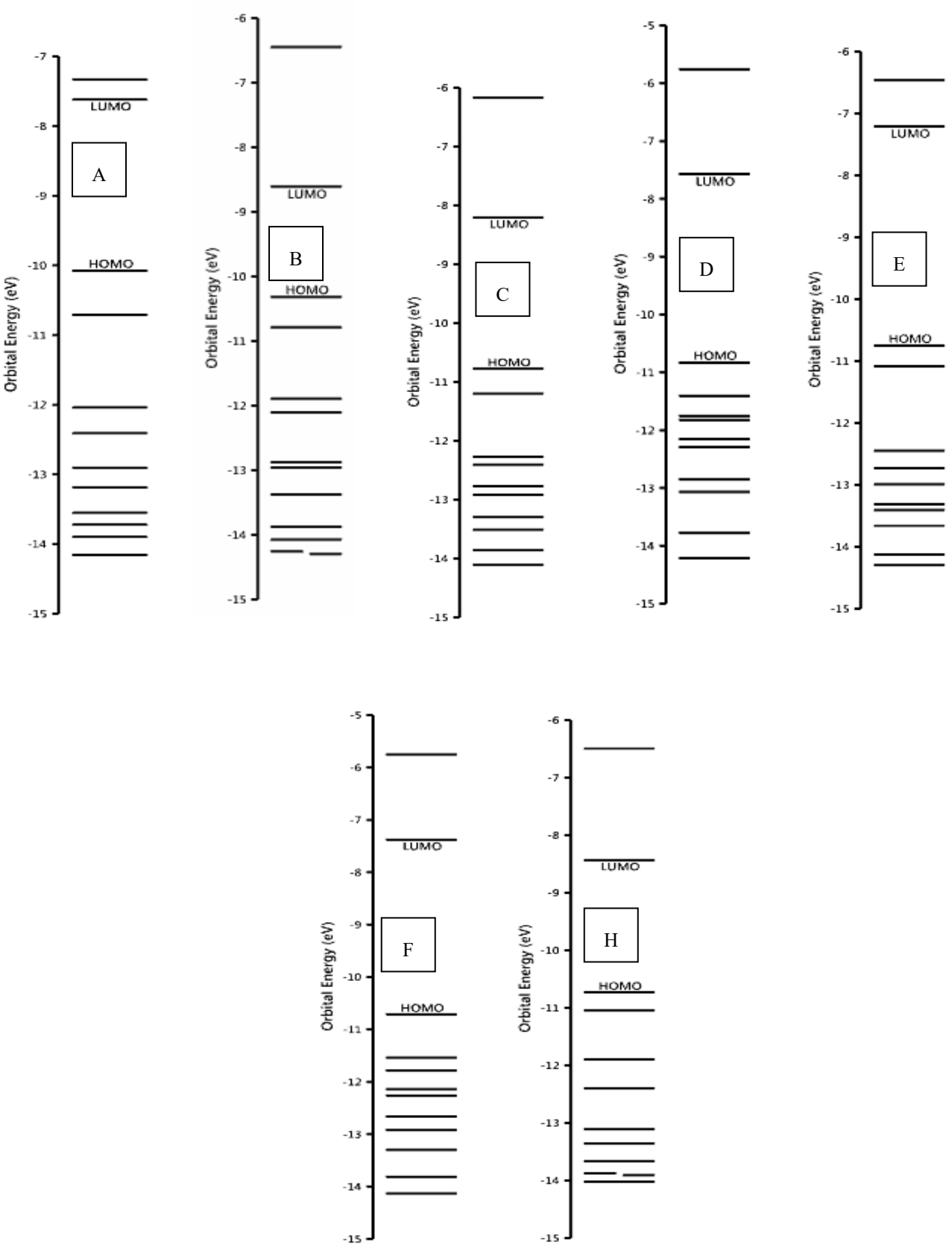

Figure 8. Some of the molecular orbital energy levels of the composites.

Table 3. The HOMO, LUMO energies and Δε values of the species considered.

Species	HOMO	LUMO	Δε
A	-972.15	-735.03	237.12
B	-995.61	-830.70	164.91
C	-1039.92	-791.69	248.23
D	-1045.28	-730.59	314.69
E	-1037.19	-695.60	341.59
F	-1033.79	-711.80	321.99
H	-1035.36	-813.53	221.83

Energies in kJ/mol.

The data of Table 3 reveal that in contrast to the HOMO energy levels, the LUMOs exhibit scatter in values. It should arise from the overall perturbational effect due to the location of the heteroatoms in the conjugation and the effect of nitronium around the organic component. Consequently, Δε values (frontier molecular orbital energy gap) show some scatter.

Figure 9 shows the HOMO and LUMO patterns of the species considered. They generally possess π-symmetry. The phenanthrene part is the main contributor of the HOMO and LUMO. In case of structure-H contribution of the nitronium component becomes appreciable.

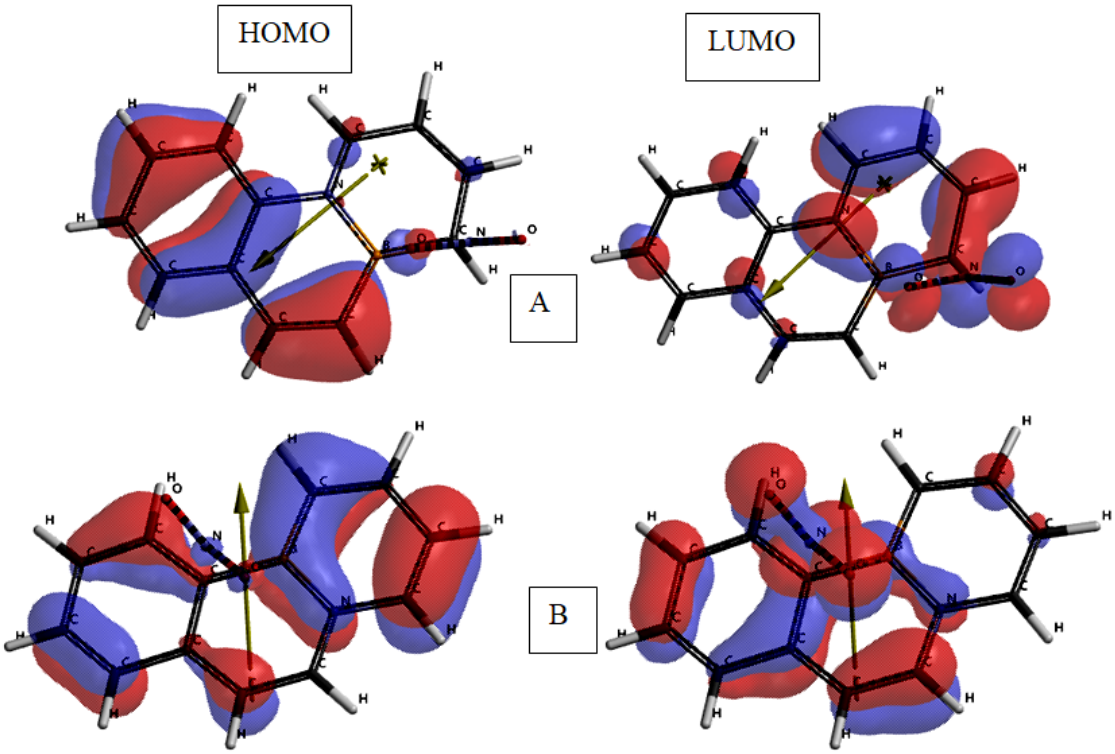

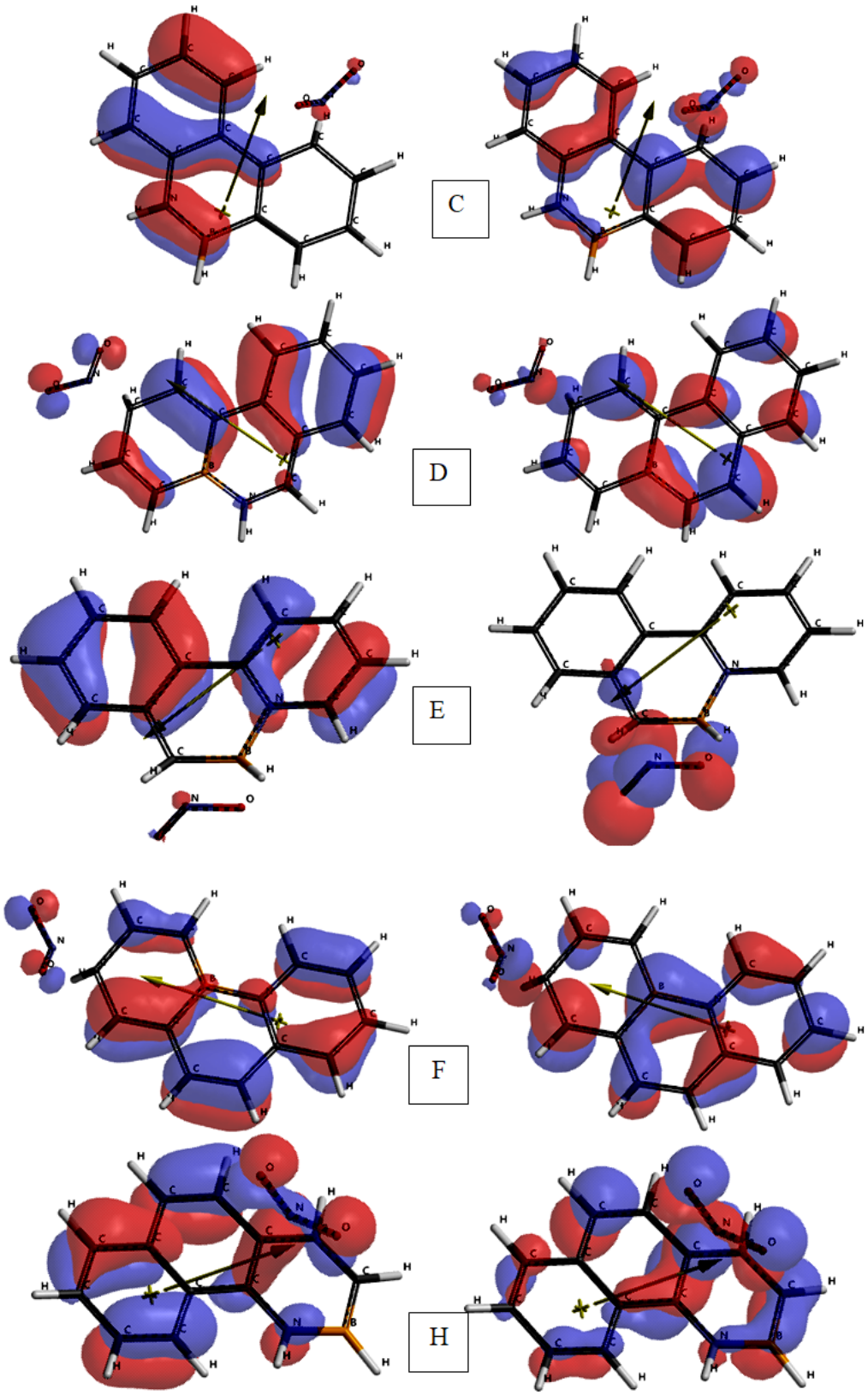

Figure 9. The HOMO and LUMO patterns of the species considered.

As an overall, the HOMO and LUMO are greatly affected by the position of the B-N bond in the conjugation which implicitly governs some other properties as well.

Figure 10 shows the UV-VIS (time dependent density functional) spectrums of the species considered. Most of the spectrums have many shoulders and peaks. The calculated intensities of the peaks are related to magnitudes of the electronic transition moments between the orbitals involved in the transitions which vary from structure to structure [24,25].

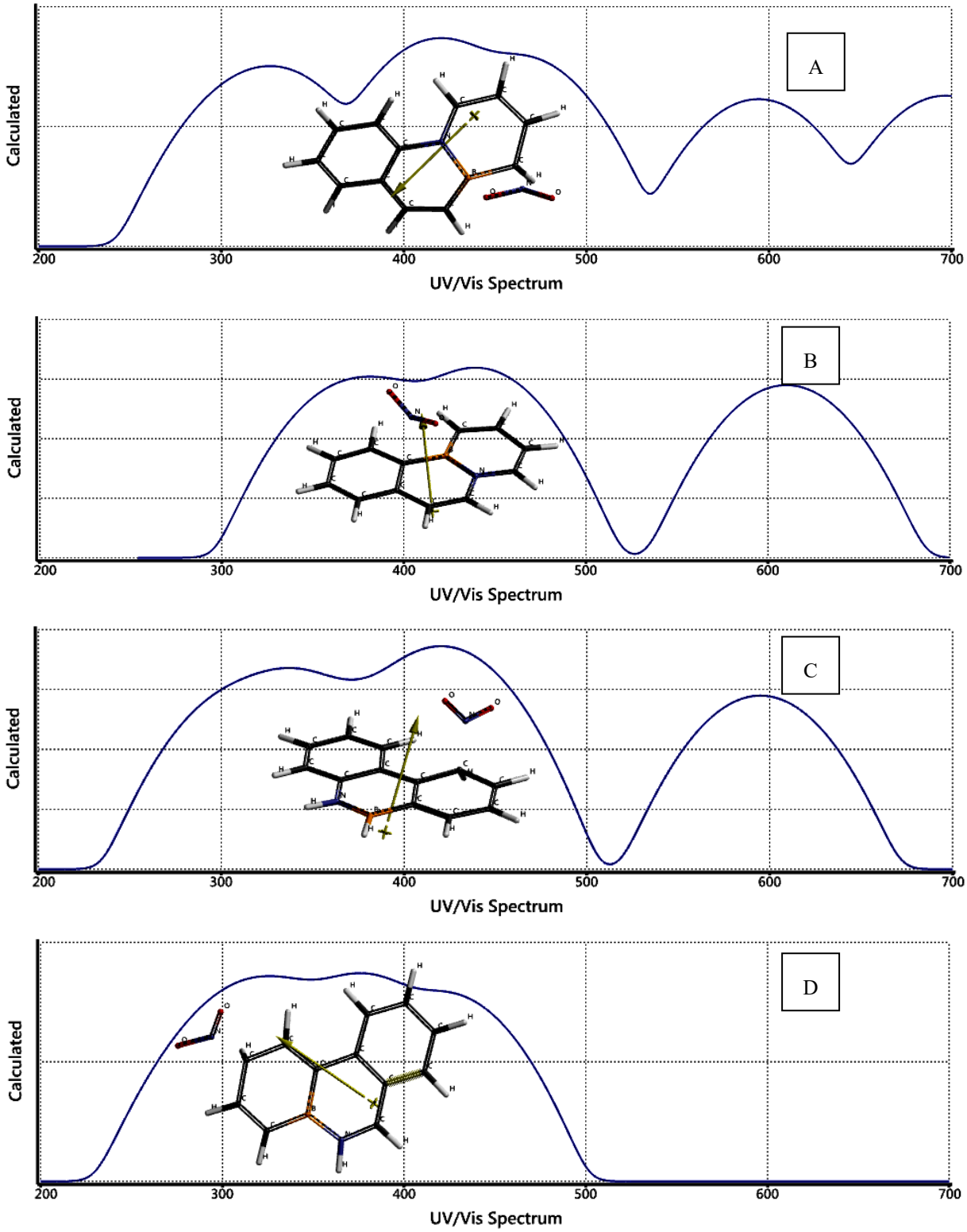

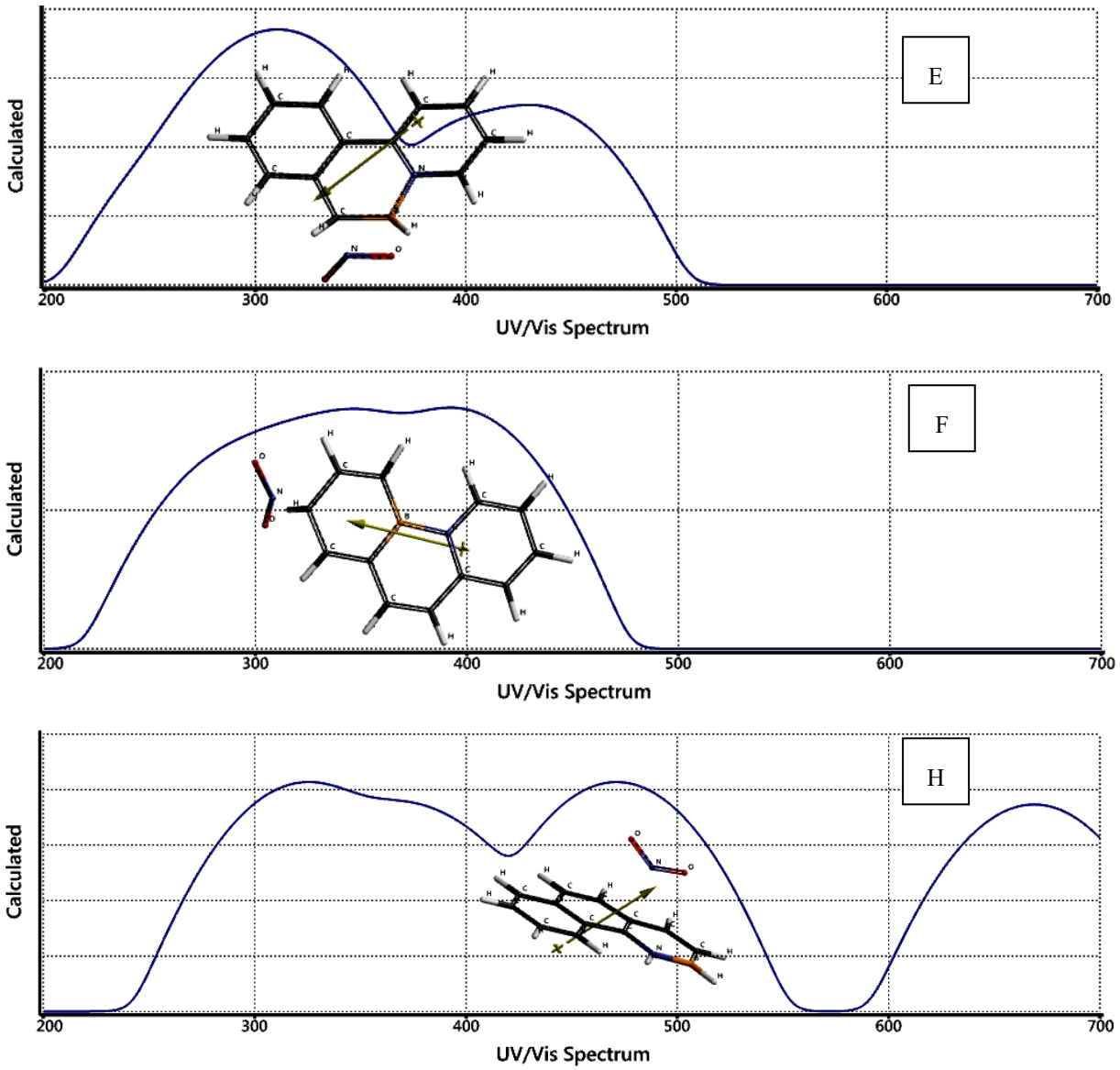

Figure 10. The UV-VIS spectrums of the species considered.

Table 4 lists the λ_{max} values and intensities of the peaks of the spectrums of species of interest.

Species	λ_{max} (nm)
A	330.12(0.024), 419.83(0.162), 463.72(0.057), 594.27(0.004), 6.96.55(0.005)
B	396.88(0.017), 439.84(0.060), 610.13(0.022)
C	330.88(0.004), 339.62(0.092), 420.45(0.379), 594.94(0.022)
D	301.84(0.005), 319.97(0.103), 377.03(0.160), 421.86(0.054)
E	306.02(0.058), 311.56(0.301), 433.97(0.007)
F	294.52(0.013), 322.55(0.061), 349.63(0.131), 393.59(0.159),
H	366.13(0.027), 385.68(0.009), 471.27(0.092), 668.88(0.030)

Intensities are in parenthesis

Table 5 lists some calculated properties of the structures considered. The dipole moment values of the species are the vectorial sum of bond dipoles which is dependent on the charges and bond lengths and note that among the structures considered, structure-H has the minimum whereas structure-D has the maximum value of the dipole moment.

The polarizability is defined according to a multivariable formula [26] which is the functions of van der Waals volume and hardness, respectively. The later one is dictated by energies of the highest occupied (HOMO) and the lowest unoccupied (LUMO) molecular orbitals [19]. The polarizability values scatter in a narrow range in contrast to the dipole moments (Table 5).

Table 5. Some properties of the species considered.

Species	Dipole (debye)	Polarizability	Cv (J/mol^o)
A	4.20	59.00	171.11
B	2.00	59.64	172.38
C	3.93	59.12	169.75
D	7.46	58.91	169.35
E	2.41	58.69	167.58
F	7.31	59.01	169.09
H	1.43	59.42	173.48

Polarizabilities in 10^{-30} m^3 units.

4. Conclusion

Interaction of nitronium ion and phenanthrene isomers having B-N bond in their π-conjugation has been subjected to DFT treatment at the level of B3LYP/6-31++G(d,p). The species of interest have exothermic heats of formation and favorable Gibbs free energy of formation values and are thermally favored and electronically stable at the standard states. Except in the cases of structures-B and -H, there exist some sorts of strong bonding interactions between the nitronium ion and the B-N bond possessing phenanthrene isomer. In structures-A and -E, the interaction is in a bicentric manner with the organic moiety, and both the nitrogen and oxygen ends of the nitronium ion are involved. Most of the properties of the species, including molecular orbital energy and UV-Vis spectra are overall topology dependent and do not obey any order.

References

[1] Huang, J., & Li, Y. (2018). BN embedded polycyclic π-conjugated systems: Synthesis, optoelectronic properties, and photovoltaic applications. *Frontiers in Chemistry, 6*, Article 341. https://doi.org/10.3389/fchem.2018.00341

[2] Cid, J., Carbó, J. J., & Fernández, E. (2012). Disclosing the structure/activity correlation in trivalent boron-containing compounds: A tendency map. *Chemistry – A European Journal, 18*(40), 12794–12802. https://doi.org/10.1002/chem.201200987

[3] Liu, Z.-Q., Fang, Q., Wang, D., Xue, G., Yu, W.-T., Shao, Z.-S., & Jiang, M.-H. (2003). Trivalent boron as acceptor in D–π-A chromophores: Synthesis, structure and fluorescence following single- and two-photon excitation. *Chemical Communications, 38*(23), 2900–2901. https://doi.org/10.1039/B207210F

[4] Giustra, Z. X., & Liu, S.-Y. (2018). The state of the art in azaborine chemistry: New synthetic methods and applications. *Journal of the American Chemical Society, 140*(4), 1184–1194. https://doi.org/10.1021/jacs.7b09446

[5] Berionni, G. (2021). Future prospects in boron chemistry: New boron compounds and Lewis acids for catalysis and materials science. *Chemical Synthesis, 1*(1), Article 10. https://doi.org/10.20517/cs.2021.11

[6] Liu, Z.-Q., Fang, Q., Wang, D., Cao, D.-X., Xue, G., Yu, W.-T., & Lei, H. (2003). Trivalent boron as an acceptor in donor-π-acceptor-type compounds for single- and two-photon excited fluorescence. *Chemistry – A European Journal, 9*(20), 5074–5084. https://doi.org/10.1002/chem.200304833

[7] Türker, L. (2002). Borazine embedded corannulenes—AM1 treatment. *Journal of Molecular Structure: THEOCHEM, 584*(1–3), 135–141. https://doi.org/10.1016/S0166-1280(02)00012-X

[8] Türker, L. (2026). A heterofullerene cap having trivalent boron – A DFT treatment. *Earthline Journal of Chemical Sciences, 13*(1), 87–98. https://doi.org/10.34198/ejcs.13126.07.087098

[9] Edel, K., Yang, X., Ishibashi, J. S. A., Lamm, A. N., Maichle-Mössmer, C., Giustra, Z. X., Liu, S.-Y., & Bettinger, H. F. (2018). The Dewar isomer of 1,2-dihydro-1,2-azaborinines: Isolation, fragmentation, and energy storage. *Angewandte Chemie International Edition, 57*(19), 5296–5300. https://doi.org/10.1002/anie.201712683

[10] Burford, R. J., Li, B., Vasiliu, M., Dixon, D. A., & Liu, S.-Y. (2015). Diels–Alder reactions of 1,2-azaborines. *Angewandte Chemie International Edition, 54*(27), 7823–7827. https://doi.org/10.1002/anie.201503483

[11] Stewart, J. J. P. (1989). Optimization of parameters for semi-empirical methods I. *Journal of Computational Chemistry, 10*(2), 209–220. https://doi.org/10.1002/jcc.540100208

[12] Stewart, J. J. P. (1989). Optimization of parameters for semi-empirical methods II. *Journal of Computational Chemistry, 10*(2), 221–264. https://doi.org/10.1002/jcc.540100209

[13] Leach, A. R. (1997). *Molecular modeling: Principles and applications*. Longman.

[14] Kohn, W., & Sham, L. J. (1965). Self-consistent equations including exchange and correlation effects. *Physical Review, 140*(4A), A1133–A1138. https://doi.org/10.1103/PhysRev.140.A1133

[15] Parr, R. G., & Yang, W. (1989). *Density-functional theory of atoms and molecules*. Oxford University Press.

[16] Becke, A. D. (1988). Density-functional exchange-energy approximation with correct asymptotic behavior. *Physical Review A, 38*(6), 3098–3100. https://doi.org/10.1103/PhysRevA.38.3098

[17] Vosko, S. H., Wilk, L., & Nusair, M. (1980). Accurate spin-dependent electron liquid correlation energies for local spin density calculations: A critical analysis. *Canadian Journal of Physics, 58*(8), 1200–1211. https://doi.org/10.1139/p80-159

[18] Lee, C., Yang, W., & Parr, R. G. (1988). Development of the Colle-Salvetti correlation energy formula into a functional of the electron density. *Physical Review B, 37*(2), 785–789. https://doi.org/10.1103/PhysRevB.37.785

[19] Wavefunction, Inc. (2006). Spartan'06. Wavefunction, Inc.

[20] Dewar, M. J. S., & Dougherty, R. C. (1975). *The PMO theory of organic chemistry*. Plenum Press.

[21] Streitwieser, A., Jr. (1961). *Molecular orbital theory for organic chemists*. John Wiley & Sons.

[22] Türker, L. (2026). Some isomers of BN-embedded phenanthrene – A DFT treatment. *Earthline Journal of Chemical Sciences, 13*(1), 43–63. https://doi.org/10.34198/ejcs.13126.04.043063

[23] Wavefunction, Inc. (2006). Trident: Molecular modeling for medicinal chemists. Wavefunction, Inc.

[24] Turro, N. J. (1991). *Modern molecular photochemistry*. University Science Books.

[25] Anslyn, E. V., & Dougherty, D. A. (2006). *Modern physical organic chemistry*. University Science Books.

[26] Abengózar, A., García-García, P., Fernández-Rodríguez, M. A., Sucunza, D., & Vaquero, J. J. (2021). Recent advances in the chemistry of BN-isosteres of polycyclic aromatic hydrocarbons. In E. F. V. Scriven & C. A. Ramsden (Eds.), *Advances in Heterocyclic Chemistry* (Vol. 135, pp. 197–275). Academic Press. https://doi.org/10.1016/bs.aihch.2020.10.005